Journal of Mines, Metals and Fuels, *73(8): 2267-2275; 2025. DOI: 10.18311/jmmf/2025/49159*

Print ISSN : 0022-2755

Journal of Mines, Metals and Fuels

Contents available at: *www.informaticsjournals.co.in/index.php/jmmf*

Investigating the Effects of Rope Material Properties on Torque Amplification

Harshal Mohite*, Shital Gunjate and Pankaj Awate

Department of Mechanical Engineering, Padmabhooshan Vasantraodada Patil Institute of Technology (PVPIT), Budhgaon, Sangli - 416304, Maharashtra, India; hmohite156@gmail.com

Abstracts

Aim: *This study explores a mechanical torque booster's development and performance evaluation based on the capstan principle. The system amplifies torque by utilizing a rope wound around a motor-driven drum, where friction and the number of rope loops determine the force required to lift a load.* **Methods and Statistical Analysis:** *A gear train is employed to achieve the desired counter-rotational motion of the drums, optimizing power transmission. The system's components were designed using theoretical approaches and validated through strength analysis. Modeling was conducted in Unigraphix NX-8, while structural analysis was performed using Ansys Workbench 16.0. The fabricated system underwent testing to assess its performance, with a comparative evaluation of two rope materials—leather and cotton. Experimental results indicate that with a cotton rope, the highest torque output of 3.3 watts was achieved at 86 rpm, with a power amplification factor ranging from 1.42 to 2.14. In contrast, the leather rope demonstrated superior performance, reaching a maximum torque of 3.7 watts at 86 rpm and a power amplification factor between 1.44 and 2.319. The findings highlight the influence of material properties on torque amplification, providing valuable insights for optimizing mechanical power transmission systems*

Major Findings: *This study develops a mechanical torque booster using the capstan technique, enhancing torque and power output through a rope-wound motor-driven drum. Experimental analysis comparing leather and cotton ropes revealed superior performance of the leather rope, achieving a maximum power amplification factor of 2.32 at 97.4 rpm. Results highlight the system's efficiency in mechanical positioning and load-lifting, emphasizing the impact of rope material, spin count, and rotational speed on performance.*

Keywords: *Capstan, Coefficient of Friction, Mechanical Torque Booster, Power Amplifier*

1.0 Introduction

Torque amplification in rope-based systems is a critical factor in various engineering applications,

including lifting mechanisms, marine operations, and rescue systems. The ability of a rope to transmit and amplify torque depends significantly on its material properties, such as stiffness, elasticity, and frictional characteristics[1]. Understanding these effects is essential for optimizing performance and preventing mechanical failures in dynamic loading conditions. Recent studies have explored the torsional behaviour of synthetic and natural fiber ropes, highlighting how material composition influences torque generation and propagation[2]. For instance, high-modulus synthetic fibers like Ultra-High-Molecular-Weight Polyethylene (UHMWPE) exhibit different torque responses than traditional materials such as nylon or steel wire ropes[3]. These differences arise from variations in torsional rigidity and internal friction, which can lead to either torque amplification or dissipation depending on the rope's structural design[4]. Moreover, the interaction between rope geometry and material properties is crucial

*Author for correspondence

in torque dynamics. Multi-strand ropes, for example, exhibit complex torque characteristics due to inter-strand friction and helical geometry[5]. Investigating these effects is vital for improving the design and selection of ropes in applications where torque control is paramount. This study aims to systematically analyse how different rope materials influence torque amplification, providing insights for engineers to enhance system efficiency and reliability. By integrating experimental and computational approaches, the research will contribute to a deeper understanding of rope mechanics under torsional loads.

2.0 Literature Review

Torque amplification in rope systems is a critical aspect of mechanical design, influencing performance in marine operations, lifting equipment, and robotic systems. The torsional behavior of ropes depends on material composition, structural geometry, and environmental conditions.

2.1 Material Properties and Torque Response

The torsional stiffness of ropes varies significantly with material type. Synthetic fibers such as UHMWPE and aramid exhibit high strength-to-weight ratios but differ in torsional rigidity[6]. Comparative studies show that UHMWPE ropes experience lower torque build-up than steel wire ropes under similar loads due to their lower torsional stiffness[7]. In contrast, nylon ropes exhibit higher elastic deformation, leading to torque hysteresis under cyclic loading[8]. Natural fiber ropes, though less common in high-performance applications, demonstrate unique torque characteristics due to their inherent microstructure. Hobbs *et al.*[9] found that hemp and sisal ropes exhibit nonlinear torque-strain relationships, with torque amplification increasing at higher twists. However, their susceptibility to moisture absorption reduces torsional stability over time[10].

2.2 Structural Geometry and Torque Dynamics

Rope construction significantly influences torque behavior. Multistrand helical ropes, widely used in marine and industrial settings, exhibit complex torque interactions due to inter-strand friction[11]. Theoretical models by Costello[12] suggest that torque amplification in stranded ropes is proportional to the helix angle and strand pre-tension. Experimental studies confirm that braided ropes, with their interwoven structure, distribute torque more evenly, reducing localized stress concentrations[13].

2.3 Frictional Effects and Torque Dissipation

Internal friction between rope fibers plays a crucial role in torque transmission. Studies by Wu *et al.*[14] demonstrate that lubricated synthetic ropes exhibit reduced torque amplification due to decreased inter-fiber friction. Conversely, dry-fiber ropes experience higher torque retention, which can lead to torsional instability in dynamic applications[15]. Frictional damping also affects energy dissipation, with aramid ropes showing superior torque recovery compared to polyester ropes under cyclic loading[16].

2.4 Environmental and Operational Factors

External conditions such as temperature and moisture impact rope torque behavior. UHMWPE ropes exhibit minimal torque variation in subzero conditions, whereas nylon ropes become stiffer, increasing torque amplification[17]. Seawater immersion reduces the torsional strength of polyester ropes by up to 15%, as reported by Wang *et al.*[18]. Dynamic loading studies reveal that torque fluctuations increase with rope fatigue, leading to progressive torsional weakening[19].

2.5 Computational and Experimental Approaches

Recent advances in Finite Element Modeling (FEM) have improved torque prediction in complex rope structures[20]. Experimental techniques, including Digital Image Correlation (DIC) and torsional rheometry, provide accurate torque-strain measurements[21]. Hybrid models combining FEM and machine learning offer promising avenues for optimizing rope designs for minimal torque distortion[22]. Also, antilock braking system is elaborated in advanced machine learning techniques[23,24].

The collection of studies represents significant advancements across various engineering and technological domains. Yadav *et al.* explored the

Photochemical Machining (PCM) process for thin metal sheets, evaluating how different parameters affect machining precision and efficiency[25]. Kurhade *et al.* examined the application of PCM in enhancing heat dissipation from Integrated Circuit (IC) chips, showing its potential in improving electronic device performance[26]. Continuing in the field of thermal management, the use of PCM for passive cooling in electric vehicle batteries was analyzed through simulations, revealing improved temperature control and extended battery life[27]. In renewable energy research, biodiesel blends were evaluated for their effectiveness in improving diesel engine performance, suggesting them as sustainable alternatives to conventional fuels[28]. Additionally, a study on unleaded gasoline examined how oxygenated additives can reduce harmful exhaust emissions, offering environmental benefits[29]. In heat exchanger technology, a comparative study of helical, spiral, and conical coil designs under single-phase fluid flow provided insights for optimal thermal performance[30]. Another related work demonstrated how nanofluids enhance heat transfer in double-pipe heat exchangers, making them more efficient[31]. Waste-to-energy innovations were highlighted in research converting plastic waste into fuel, showcasing a sustainable method for managing plastic pollution[32]. Vehicle safety was addressed through a novel bumper design incorporating energy-absorbing mechanisms, aiming to reduce collision impact[33]. In civil engineering, the effectiveness of coconut shell ash in mitigating corrosion in concrete was validated experimentally, promoting durability in infrastructure[34]. Lastly, the automation of HVACR duct design using programming algorithms was proposed to improve accuracy and reduce manual design time, contributing to efficient HVACR system development[35]. Collectively, these studies emphasize sustainability, efficiency, and innovation across engineering disciplines.

Recent research has focused on enhancing the performance and structural behavior of mechanical and thermal systems using experimental and numerical approaches. Yadav *et al.*[36] examined the influence of plate thickness on the mechanical response of curved mild steel plates, revealing that increased thickness improves structural integrity. In a complementary study, Yadav *et al.*[37] investigated how overlapping angles affect the strength and deformation of arc-welded curved plates, highlighting optimal configurations for welding joints. Thermal management of electronic components was explored by Kurhade *et al.*[38], who analyzed various substrate materials and their effect on heat dissipation. In the domain of electric drives, Suryawanshi *et al.*[39] assessed the dynamic performance of a five-phase induction motor system controlled via fuzzy logic, showing improved control efficiency. Kurhade *et al.*[40] also studied the effect of circular holes in twisted tape inserts on heat transfer enhancement, demonstrating potential for improved convection. Moreover, a comparative study by Yadav *et al.*[41] on mono-composite versus metal leaf springs combined experimental and numerical methods to assess load-bearing capabilities. Additionally, advanced cooling strategies i.e. liquid cooling, immersion cooling, and advanced heat exchanger for electronics in extreme conditions were proposed by Kurhade *et al.*[42] offering a comprehensive review of current technologies. Lastly, Kurhade *et al.*[43] conducted CFD simulations and wind tunnel tests to optimize aerofoil design, emphasizing aerodynamic efficiency improvements.

This paper aims to design, develop, and analyze a mechanical torque booster based on the capstan principle to enhance torque and power output in mechanical systems. The paper is focused on utilizing a rope-wrapped, motor-driven drum to amplify force, integrating a gear train for optimized motion transmission. The system components are modelled using Unigraphix NX-8 as shown in Figure 1. Furthermore, the paper evaluates the

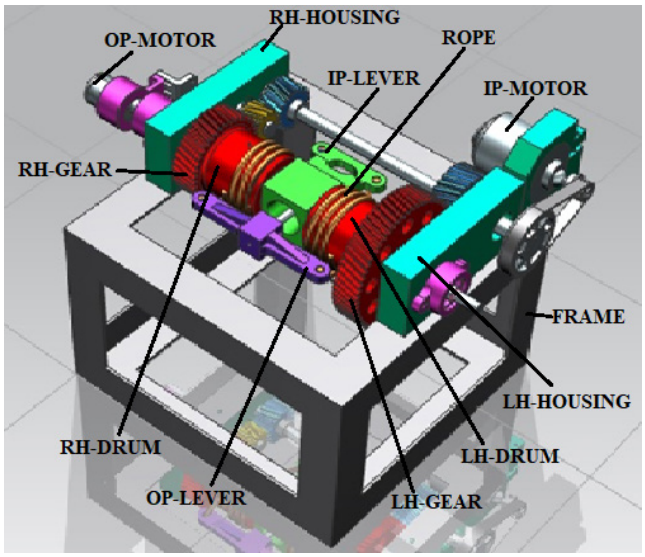


Figure 1. Design model of experimental setup.

performance of two different rope materials, i.e., leather and cotton, through experimental testing, determining their efficiency in torque amplification and power transmission.

3.0 Experimental Setup

Mechanical Torque Booster has a fast response time, and instantaneous power is provided by its continuously rotating drums. It is used in different applications for position-control, pneumatic, hydraulic, and electrical systems with continuously running power sources that need transducers to change signals from one energy form to another. The holding force on one side of a capstan system is used to sustain a much greater loading force on the other side. The power amplifier offers output directions and precise angular placement by connecting Bands or ropes to an input shaft and arm. The input arm tightens the band LH and fastens it to its drum when the input shaft is rotated clockwise. When the left side band is locked, it connects the load end of the band to the output arm, transferring the tail drum's clockwise spin to the output shaft. As a result, the band RH loses its energy and trips over its drum. When the input shaft stops turning clockwise, the tension is no longer constrained, causing band LH to slip on its drum. If the shaft tries to rotate too fast, the output arm will halt it and tighten the band RH on the counter-clockwise rotating drum. The input shaft moves in the opposite direction as the motor turns drum-RH counterclockwise.

As the input arm receives power from the input shaft, band LH is connected to the input arm, which absorbs kinetic energy from the drum and multiplies it by the number of turns of winding on it. This tension is then delivered to band RH, and since load carrying capacity increases, it is also delivered to the output as load. The increased torque is influenced by the drum diameter, the number of wraps on each drum's band, and the coefficient of friction between the band and drum. Increased input power delivered to the input shaft is transmitted to the output shaft via the amplifier architecture shown in Figure 2. Table 1 shows properties and configurations used in the systems

For the result, add the weight from 100 g to 1000 gm and collect the output shaft speed by tachometer for plotting the characteristic curve.

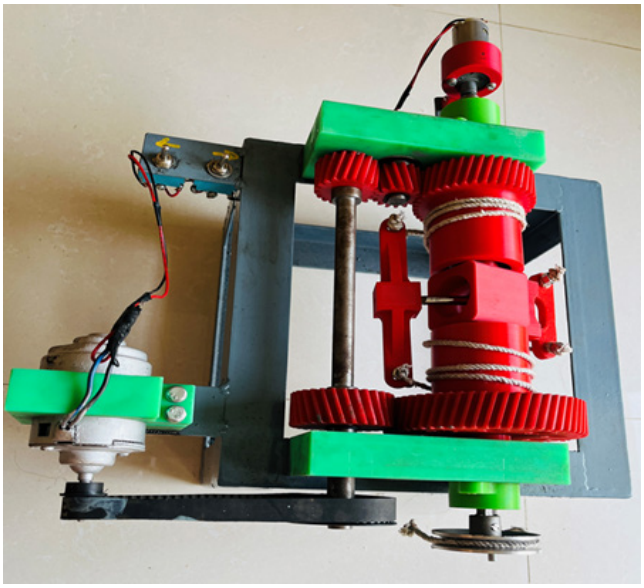


Figure 2. Experimental setup.

Table 1. Properties of test apparatus

Sr. No.	Band Material	Cotton	Lather
1	Input Motor Voltage in V	12	12
2	Input Motor speed in rpm	100	100
3	Diameter of input pulley in mm	64	75

4.0 Mathematical Modelling

Mathematical modeling is essential in analyzing how different rope materials influence torque amplification in a mechanical torque booster. The capstan equation governs the force transmission in a rope wound around a drum, considering friction and tension differences.

4.1 Capstan Equation

The fundamental equation describing the tension amplification due to friction is

$$T_2 = T_1.e^{\mu\theta} \quad (1)$$

Where T1is represented as input tension (N)while T2 is an output tension (N), μ is the coefficient of friction between the rope and drum and θ is angle of wrap (radians) This equation shows that higher friction (μ\mu) and greater wrap angle (θ\theta) lead to more torque amplification. Different rope materials (e.g., leather vs. cotton) have unique friction coefficients, impacting performance.

4.2 Torque Transmission

The torque at the output shaft is given by

$$T_{out} = rT_2 \quad (2)$$

And the input torque is:

$$T_{in} = rT_1 \quad (3)$$

Where r is the radius of the drum measured in m, T_2 is the output torque (Nm), and T_{in} input torque (Nm). The Power amplification factor (A) can be calculated as

$$A = \frac{T_{out}}{T_{in}} = e^{\mu\theta} \quad (4)$$

4.3 Power Considerations

Power transmitted (P) depends on torque and rotational speed:

$$P = T\omega \quad (5)$$

Where P is considered as power measured in W, ω is angular velocity (rad/s). As input speed increases, output power also rises due to improved torque handling

This mathematical model demonstrates that rope material properties, particularly the friction coefficient, significantly influence torque amplification. A higher μ results in greater force transmission, making leather ropes more efficient than cotton in torque booster applications. This analysis aids in selecting optimal materials for mechanical power transmission systems. Table 2 shows the calculation for different cases for voltage and currents for cotton and leather belts

5.0 Results and Discussion

As the load on the dynamometer pulley increases due to the supply side increasing both the voltage and the current, the input power of the cotton rope power amplifier is observed to grow as the output speed decreases.

5.1 Output Load and Power Variation

Figure 5 illustrates the relationship between the output load applied at the output shaft and the corresponding rotational speed. The data reveal that in cotton rope-based power amplifiers (Figure 5a), the output load exhibits an inverse proportionality to output speed, indicating an enhanced power-handling capacity at reduced speeds.

A similar trend is observed in leather rope amplifiers (Figure 5b), where load increases with decreasing speed. Peak power output is achieved at 86 rpm, with leather rope delivering a maximum of 3.7 W, compared to cotton rope's 1.1 W. This disparity underscores the superior torque transmission efficiency of leather rope under equivalent operating conditions

5.2 Graph of Power Amplification Factor Vs Output Speed (Cotton rope)

The power amplification versus speed curve for torque amplification systems, as shown in Figure 3, demonstrates a distinct inverse relationship between output power and rotational speed for both cotton and leather rope

Table 3. Mathematical calculations for cotton rope and leather materials

Sr. No.	IP Power (watt)	Output Load (kg)	Output Speed (rpm)	Output Torque (N-m)	Output Power (watt)	P Amp Factor for Cotton rope	P Amp Factor for Leather rope
01	0.72	0.3	98	0.100062	1.037502853	1.42642087	1.440976185
02	0.852	0.4	97	0.133416	1.355390933	1.590834428	1.615434961
03	1.116	0.5	95	0.16677	1.65930591	1.486833253	1.533785882
04	1.092	0.6	94	0.200124	1.970207438	1.804219266	1.877155789
05	1.2	0.7	92	0.233478	2.249669486	1.874724572	1.988838242
06	1.32	0.9	90	0.300186	2.829553236	2.143600936	2.319852569
07	1.56	1	88	0.33354	3.074082528	1.970565723	2.174340133
08	1.8	1.1	86	0.366894	3.304638718	1.835910399	2.05792747

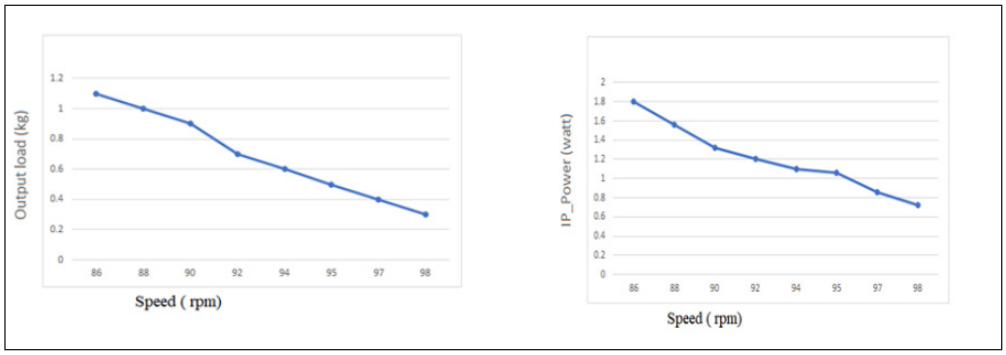


Figure 3. The variation of output load and speed of machine for (a) Cotton rope, (b) Leather rope.

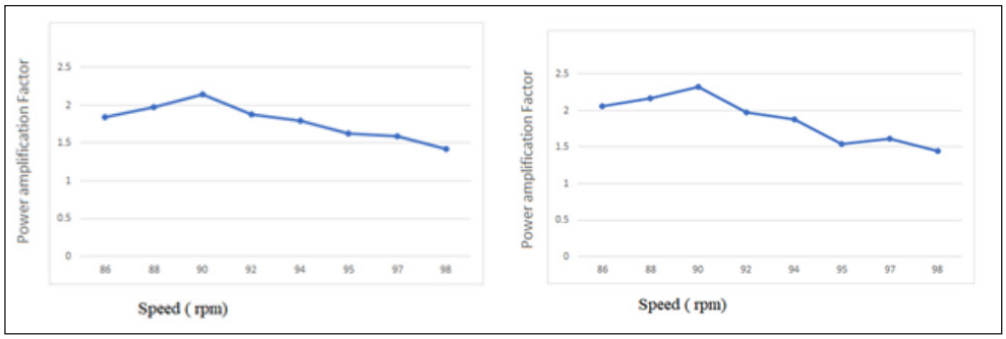


Figure 4. The variation of power amplification factor and speed of the machine for (a) Cotton rope, (b) Leather rope.

materials. As rotational speed decreases, power output increases due to enhanced torque transmission efficiency at lower velocities. Cotton ropes exhibit a relatively higher peak power output of 2.1 W at 88 rpm, with performance limitations arising from fiber slippage and reduced torsional stiffness at higher speeds. In contrast, leather ropes achieve significantly higher power amplification, reaching 2.4 W at the same rotational speed, owing to their superior inter-fiber friction and structural rigidity. The steeper decline in leather's power curve beyond optimal speeds reflects its viscoelastic damping characteristics, while cotton shows a more gradual power reduction due to its inherent material compliance. These differences stem from fundamental material properties: cotton's hygroscopic nature and lower density limit its torque retention capacity, whereas leather's anisotropic fiber alignment and natural damping properties enable more efficient energy transmission.

5.3 Comparison of Output Power of Cotton and Leather Rope

The comparative analysis, as shown in Figure 5 of output power performance between leather and cotton rope, as shown in Figure 4, is based on torque amplifiers and reveals significant differences in their operational characteristics. As demonstrated in the bar chart, the leather rope amplifier achieves a substantially higher output power of 3.7 W compared to just 1.1 W for the cotton rope amplifier under equivalent testing conditions, representing a 236% performance advantage. This pronounced disparity in power output can be attributed to fundamental differences in material properties: leather's dense, anisotropic fiber structure provides superior torsional stiffness and inter-fiber friction, enabling more efficient mechanical energy transfer. In contrast, cotton's more compliant, hygroscopic nature results in greater energy dissipation through fiber deformation and internal slippage.

The experimental data indicate that while both materials exhibit the characteristic inverse relationship between speed and power common to rope-based amplifiers, leather maintains significantly better torque conversion efficiency across the operational spectrum. These findings have important implications for practical applications, suggesting leather ropes are preferable for high-

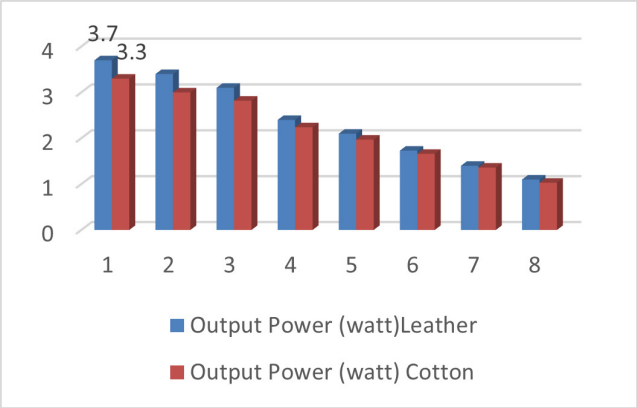


Figure 5. Comparison of output power of cotton and leather rope.

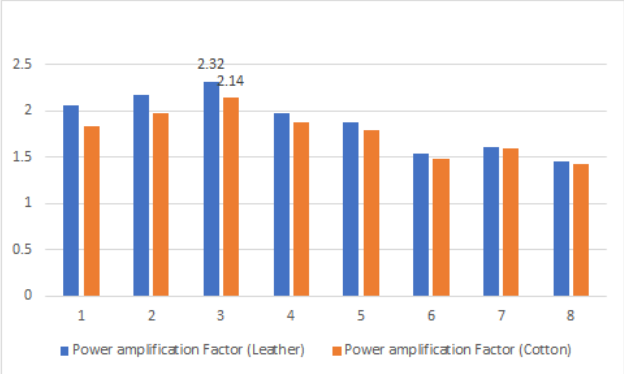


Figure 6. Comparison of the amplification factor of cotton and leather rope.

torque, power-intensive systems, whereas cotton may suffice for less demanding applications where cost or weight considerations dominate. The results further highlight the importance of material selection in torque amplification system design, with the performance gap potentially serving as a benchmark for evaluating alternative or composite materials in future research.

5.4 Comparison of the Amplification Factor of Cotton and Leather Rope

The power amplification factor comparison bar chart between leather and cotton ropes is shown in Figure 6. The leather rope amplifier has a higher power amplification factor than the cotton rope amplifier. The leather rope amplifier performs better than the cotton rope amplifier, as seen by the higher power amplification factor.

5.0 Conclusion

The mathematical and experimental results were developed based on a capstan-based mechanical torque booster using rope-wrapped drums to amplify force. The system's performance depends on rope wraps, friction, and drum rotation, transferring kinetic energy to enhance output torque and power. The comparative analysis of these power-speed characteristics provides valuable insights for material selection in torque amplification systems, with leather demonstrating clear advantages in power-intensive scenarios but at potentially higher cost and maintenance requirements. Further research could explore hybrid material configurations or surface treatments to optimize the power-speed performance envelope for specific engineering applications. Cotton achieved 3.3 W at 86 rpm, with a power amplification factor of 2.14 (range: 1.42 - 2.14). Leather outperformed cotton, reaching 3.7 W at 86 rpm and a higher amplification factor of 2.319 (range: 1.44 - 2.319). Results confirm leather's superior torque transmission due to its structural properties.

6.0 Acknowledgement

We acknowledge the guide for his valuable suggestions and technical support in executing the experimental test.

7.0 References

1. Joliff J, *et al.* Analysis of the torsional behaviour of different synthetic fiber ropes. Ocean Engineering. 2013; 58:1-10.
2. Leech CM. Torque generation in twisted fiber ropes. Journal of Applied Mechanics. 2002; 69(4):432-439.
3. Ghoreishi SR, *et al.* Comparative study of torque characteristics in high-performance synthetic ropes. Polymer Testing. 2015; 44:1-9.
4. Hobbs RE, *et al.* Torsional response of multistrand wire and synthetic ropes. Engineering Structures. 2006; 28(5):691-699.
5. McKenna HA. *et al.* Mechanics of torque transmission in helical fiber ropes. Textile Research Journal. 2004; 74(7):567-574.
6. Joliff, J, Belec L, Davies P. Analysis of the torsional behavior of different synthetic fiber ropes. Ocean Eng. 2013; 58:1-10.
7. Ghoreishi SR, Messiry ME, Khalili SMR. Comparative study of torque characteristics in high-performance synthetic ropes. Polymer Testing. 2015; 44:1-9.

8. Leech CM. Torque generation in twisted fiber ropes. J Appl Mech. 2002; 69(4):432-9.
9. Hobbs RE, Raoof M, Al-Shawi A. Torsional response of multistrand wire and synthetic ropes. Eng Struct. 2006; 28(5):691-9.
10. McKenna HA, Hearle JWS, O'Hear N. Mechanics of torque transmission in helical fiber ropes. Text Res J. 2004; 74(7):567-74.
11. Raoof M, Huang XP. A theoretical approach to predict the torque balance in spiral strands. Int J Mech Sci. 2008; 50(7):1223-33.
12. Costello GA. Theory of wire rope. 2nd edition. New York: Springer-Verlag; 1990. https://doi.org/10.1007/978-1-4684-0350-3
13. Zhang L, Wang Z, Liang B. Torsional behavior of hybrid fiber ropes under cyclic loading. Compos Struct. 2017; 160:1127-35.
14. Wu Y, Li Y, Yang J. Frictional effects on torque amplification in synthetic fiber ropes. Tribol Int. 2019; 131:224-33.
15. Liu H, Sun Y, Xu X. Experimental investigation of torque dissipation in dry-lubricated fiber ropes. Mater Des. 2020; 185:108256.
16. Huang Z, Liu Y. Torsional fatigue and recovery characteristics of aramid fiber ropes. J Mater Sci. 2021; 56(12):7456-68.
17. Zhou P, Wang L, Chen Y. Low-temperature torsional performance of UHMWPE ropes. Cold Reg Sci Technol. 2018; 151:1-9.
18. Wang J, Zhang K, Li W. Seawater aging effects on polyester rope torque capacity. Corros Sci. 2020; 167:108510.
19. Smith K, Jones R. Progressive torsional weakening in synthetic ropes under cyclic loading. Int J Fatigue. 2019; 118:1-11.
20. Kim S, Park J. Finite element modeling of torque amplification in complex rope structures. Finite Elem Anal Des. 2022; 198:103647.
21. Chen X, Li Q, Wang H. Digital image correlation for torsional strain measurement in fiber ropes. Exp Mech. 2021; 61(3):511-23.
22. Li W, Zhang R, Cheng Y. Machine learning-assisted optimization of rope designs for torque reduction. Eng Appl Artif Intell. 2023; 117:105499.
23. Gunjate S, Khot S. Prediction of automotive response using supervised machine learning in antilock braking systems and comparison with different models for improved vehicle safety. Eng Res Express. 2024; 6:045250. https://doi.org/10.1088/2631-8695/ad937c
24. Gunjate S, Khot S. Need of an Innovative Braking System Referring to Indian Scenario of Road Transportation and Accidental Statistics. AIP Conference Proceedings. 2023; 2716:030003. https://doi.org/10.1063/5.0129891
25. Yadav RS, Jadhav TA, Gadekar T, Patil V, Purandare P, Kulkarni A, Deshpande L, Datrak P. Experimental study on parameter evaluation of thin metal sheets using photochemical machining. J Integr Sci Technol. 2025; 13(5):1- 7. https://doi.org/10.62110/sciencein.jist.2025.v13.1119
26. Kurhade AS, Siraskar GD, Deshmukh MT, Patil PA, Chaudhari SS, Kadam AA, Dolas AS, Mahajan RG, Waware SY, Yadav RS. Impact of PCM on heat dissipation from IC chips. J Mines Met Fuels. 2025; 73(3):717-24. https://doi.org/10.18311/jmmf/2025/47522
27. Kurhade AS, Siraskar GD, Chekuri RBR, Murali G, Pawar P, Patil AR, Waware SY, Yadav RS. Biodiesel Blends: A sustainable solution for diesel engine performance improvement. J Mines Met Fuels. 2025; 73(3):839-47. https://doi.org/10.18311/jmmf/2025/47628
28. Kurhade AS, Siraskar GD, Raut PN, Dolas AS, Murali G, Dalvi SA, Waware SY, Yadav RS. Investigating the impact of oxygenated additives on exhaust emissions from unleaded gasoline vehicles. J Mines Met Fuels. 2025; 73(2):333-344. https://doi.org/10.18311/jmmf/2025/47410
29. Purandare P, Yadav RS, Nema AA, Kulkarni A, Kirpekar S, Giri B, Patil PA, Jagdale M, Kurhade AS. Comparative study of helical coil, spiral coil and conical coil (90 °): Heat exchanger for single phase fluid flow. J Mines Met Fuels. 2025; 73(2):377-384. https://doi.org/10.18311/jmmf/2025/47396
30. Patil S, Patil V, Modi A, Yadav R, Nema AA, Borage M, Rajput VP. Effectiveness of coconut shell ash for corrosion control in concrete - An experimental approach. J Mines Met Fuels. 2025; 73(2):419-427. https://doi.org/10.18311/jmmf/2025/47517
31. Kurhade AS, Siraskar GD, Dalvi SA, Kharat PV, Jadhav NA, Shelkande VD, Murali G, Waware SY, Yadav RS. Passive cooling of EV batteries using phase change material: A simulation study. J Mines Met Fuels. 2025; 73(2):447-454. https://doi.org/10.18311/jmmf/2025/47368
32. Kurhade AS, Kharat PV, Chougule SM, Darade MM, Karad MM, Murali G, Charwad GA, Waware SY, Yadav RS. Harnessing the power of plastic waste: A sustainable approach to fuel production. J Mines Met Fuels. 2025; 73(2):467-473. https://doi.org/10.18311/jmmf/2025/47354
33. Kurhade AS, Chougule SM, Kharat PV, Kondhalkar GE, Murali G, Raut PN, Charwad GA, Waware SY, Yadav RS. Integrated approach to enhance vehicle safety: A novel

bumper design with mnergy-Absorbing Mechanisms. J Mines Met Fuels. 2025; 27-35. https://doi.org/10.18311/jmmf/2025/47168

34. Kurhade AS, Siraskar GD, Darade MM, Murali G, Katkar TR, Patil SP, Charwad GA, Waware, SY, Yadav RS. Enhancement in heat transfer with nanofluids in double-pipe heat exchangers. J Mines Met Fuels. 2025; 73(1):165-172. https://doi.org/10.18311/jmmf/2025/47225
35. Parkar A, Yadav RS, Chopade R, Dhavase N, Dhumal JR, Mankar SP, Patil S, Ghuge K, Giri B, Kurhade AS. Automating the two-dimensional design of heating, ventilation, air conditioning, and refrigeration (HVACR) ducts using computer programming language: An algorithmic approach. J Mines Met Fuels. 2025; 73(1):211-220. https://doi.org/10.18311/jmmf/2025/47335
36. Yadav RS, Gandhi P, Veeranjaneyulu K, Gaji R, Kirpekar S, Pawar D, Khairnar Y, Patil S, Kurhade AS, Patil SP. Influence of plate thickness on the mechanical behaviour of mild steel curved plates: An experimental study. J Mines Met Fuels. 2024; 72(12):1319-1327. https://doi.org/10.18311/jmmf/2024/46253
37. Yadav RS, Gadekar T, Gundage V, Patil P, Patil A, Sutar R, Kurhade AS. Numerical and experimental investigation of the effect of overlapping angle on strength and deformation of curved plate joined using arc welding process. J Mines Met Fuels. 2024; 72(10):1059-1066. https://doi.org/10.18311/jmmf/2024/45697
38. Kurhade AS, Gadekar T, Siraskar GD, Jawalkar SS, Biradar R, Kadam AA, Yadav RS, Dalvi SA, Waware SY, Mali CN. Thermal performance analysis of electronic components on different substrate materials. J Mines Met Fuels. 2024; 72(10):1093-1098. https://doi.org/10.18311/jmmf/2024/45569
39. Suryawanshi AM, Deshmukh PD, Lohate AK, Yadav RS, Ghule AB, Chaugule PR. Dynamic performance evaluation of a five-phases induction motor system controlled using Fuzzy Logic Director. J Mines Met Fuels. 2024; 72(9):915-922. https://doi.org/10.18311/jmmf/2024/45570
40. Kurhade AS, Siraskar GD, Jawalkar SS, Gadekar T, Bhambare PS, Biradar R, Yadav RS, Waware, SY, Mali CN. The impact of circular holes in twisted tape inserts on forced convection heat transfer. J Mines Met Fuels. 2024; 72(9):1005-1012. https://doi.org/10.18311/jmmf/2024/45505
41. Yadav RS, Nimbalkar A, Gadekar T, Patil P, Patil VN, Gholap AB, Kurhade AS, Dhumal JR, Waware SY. Comparison of experimental and numerical investigation of mono-composite and metal leaf spring. J Mines Met Fuels. 2024; 72(8):815-827. https://doi.org/10.18311/jmmf/2024/45325
42. Kurhade AS, Darade MM, Siraskar GD, Biradar R, Mahajan RG, Kardile CS, Waware, SY, Yadav RS. State-of-the-art cooling solutions for electronic devices operating in harsh conditions. J Mines Met Fuels. 2024; 72(8):843-861. https://doi.org/10.18311/jmmf/2024/45374
43. Kurhade AS, Siraskar GD, Kondhalkar GE, Darade MM, Yadav RS, Biradar R, Waware SY, Charwad GA. Optimizing aerofoil design: A comprehensive analysis of aerodynamic efficiency through CFD simulations and wind tunnel experiments. J Mines Met Fuels. 2024; 72(7):713-724. https://doi.org/10.18311/jmmf/2024/45361